Versatile Coordination Modes and Transformations of the Cyclooctatriene Ligand in Ru(C_8H_{10})L_3 (L = Tertiary Phosphine)

Sanshiro Komiya,* Jose Giner Planas, Koji Onuki, Zhaobin Lu, and Masafumi Hirano

Department of Applied Chemistry, Faculty of Technology, Tokyo University of Agriculture and Technology, 2-24-26 Nakacho, Koganei, Tokyo 184-8588, Japan

Received December 20, 1999

Reaction of Ru(η^4-C_8H_{12})(η^6-C_8H_{10}) (**1**) or Ru(η^4-C_8H_{11})$_2$ (**2**) with tertiary phosphines gives Ru(η^4-C_8H_{10})L_3 [L = PMe_3 (**4a**), PMe_2Ph (**4b**), PEt_3 (**4c**), PEt_2Ph (**4d**), P(n-Bu)$_3$ (**4e**)]. The cyclooctatriene moiety in **4a** oxidatively adds to the ruthenium, giving Ru(6-η^1:1−3-η^3-C_8H_{10})L_3 [L = PMe_3 (**3a**), PMe_2Ph (**3b**)]. Complexes **4c**−**e** dissociate one phosphine ligand in solution, affording the (hydrido)ruthenium complexes RuH(η^5-C_8H_9)L_2 [L = PEt_3 (**5c**), PEt_2-Ph (**5d**), P(n-Bu)$_3$ (**5e**)]. Whereas prolonged heating of **4c** at 70 °C caused disproportionation of the η^4-C_8H_{10} moiety giving a mixture of the cyclooctatetraene complex Ru(η^4-C_8H_8)(PEt_3)$_3$ (**6**) and RuH(η^5-C_8H_{11})(PEt_3)$_2$ (**7**), heating of **1** with PEt_3, **4c**, or **4d** in the presence of 1,5-C_8H_{12} at 70 °C gave Ru(η^4-bicyclo[4.2.0]octa-2,4-diene)L_3 [L = PEt_3 (**8a**), L = PEt_2Ph (**8b**)]. The molecular structures of **3b**, **4c**, **6**, and **8b** have been established by X-ray structure analysis.

Introduction

The oxidative addition chemistry of low-valent transition metal complexes has been extensively studied.[1] Among zerovalent ruthenium complexes, Ru(η^4-C_8H_{12})(η^6-C_8H_{10}) (**1**) is a widely used and highly versatile starting material in the preparation of new complexes as well as in catalysis.[2] Specifically, **1** or its isomer Ru(η^5-C_8H_{11})$_2$ (**2**) in combination with tertiary phosphine ligands has provided useful catalytic systems.[3] It has been suggested that the cyclooctatriene ligand in **1** is often replaced by appropriate ligands to give reactive species in the early stages of catalytic reactions.[1] For example, the cyclooctatriene ligand is replaced by arenes from **1** in the presence of molecular hydrogen, giving Ru(η^4-C_8H_{12})(arene).[4] Cyclooctatriene is also selectively displaced in the reaction of **1** with excess CO or dppm [dppm = 1,2-bis(diphenylphosphino)methane], affording the zerovalent complexes Ru(η^4-C_8H_{12})$(CO)_3$ or Ru_2(η^4-C_8H_{12})$_2$(η^4-C_8H_{10})$(dppm)_2$, respectively.[5,6] Although **1** was thought to generally liberate the triene ligand more easily than the diene, we recently reported that 1,5-cyclooctadiene is displaced with excess trimethylphosphine, affording the divalent Ru(6-η^1:1−3-η^3-C_8H_{10})$(PMe_3)_3$ (**3a**).[7] Mitsudo et al. have also reported the selective displacement of 1,5-cyclooctadiene in **1** by dimethyl maleate, affording Ru(η^6-C_8H_{10})(dimethyl maleate)$_2$.[2c]

Herein we wish to report that 1,5-cyclooctadiene is selectively displaced in all reactions of **1** with monodentate trialkylphosphine ligands. The cyclooctatriene ligand, which remains bonded to ruthenium, displays a variety of coordination modes that are highly dependent on the cone angle of the phosphine ligand used. A detailed account of these reactions and of extensive studies is also described.

Results and Discussion

Reactions of Ru(η^4-C_8H_{12})(η^6-C_8H_{10}) (1) and Ru(η^5-C_8H_{11})$_2$ (2) with Monodentate Tertiary Phosphines. (a) PMe_3, PMe_2Ph. As reported, complex **1** immediately reacts with PMe_3 at room temperature to form a monophosphine adduct Ru(η^4-C_8H_{12})(η^4-C_8H_{10})(PMe_3), regardless of the amount of phosphines.[6a,7] Further heating of Ru(η^4-C_8H_{12})(η^4-C_8H_{10})(PMe_3) with PMe_3 resulted in the formation of Ru(6-η^1:1−3-η^3-C_8H_{10})$(PMe_3)_3$ (**3a**).[7] A similar reaction of **1** with 3 equiv of PMe_2Ph at 50 °C for 24 h gave the divalent complex Ru(6-η^1:1−3-η^3-C_8H_{10})$(PMe_2Ph)_3$ (**3b**) in 25% yield (Scheme 1).

(1) (a) Halpern, J.; *Acc. Chem. Res.* **1970**, *3*, 368. (b) Collman, J. P.; Hegedus, L. S. *Principles and Applications of Organotransition Metal Chemistry;* University Science: Mill Valley, CA, 1980.

(2) (a) Pertili, P.; Vitulli, G. *Comments Inorg. Chem.* **1991**, *11*, 175, and references therein. (b) Zhang, S.; Mitsudo, T.; Kondo, T.; Watanabe, Y. *J Organomet. Chem.* **1993**, *450*, 197. (c) Mitsudo, T.; Suzuki, T.; Zhang, S.; Imai, D.; Fujita, K.; Manabe, T.; Shiotsuki, M.; Watanabe, Y.; Wada, K.; Kondo, T. *J. Am. Chem. Soc.* **1999**, *121*, 1839.

(3) (a) Mitsudo, T.; Nakagawa, Y.; Watanabe, K.; Hori, Y.; Misawa, H.; Watanabe, H.; Watanabe, Y. *J. Org. Chem.* **1985**, *50*, 565. (b) Mitsudo, T.; Hori, Y.; Watanabe, Y. *J. Organomet. Chem.* **1987**, *334*, 157. (c) Wakatsuki, Y.; Yamazaki, H.; Kumegawa, N.; Satoh, T.; Satoh, Y. *J. Am. Chem. Soc.* **1991**, *113*, 9604.

(4) (a) Pertici, P.; Vitulli, G.; Lazzaroni, R.; Salvadori, P. *J. Chem. Soc., Dalton Trans.* **1982**, 1019. (b) Vitulli, G.; Pertici, P.; Lazzaroni, R.; Salvadori, P. *J. Chem. Soc., Dalton Trans.* **1984**, 2255. (c) Vitulli, G.; Pertici, P.; Bigelli, C. *Gazzetta Chim. Ital.* **1985**, *115*, 79. (d) Vitulli, G.; Lazzaroni, R. *Inorg. Chim. Acta* **1988**, *149*, 235.

(5) Deganello, G.; Mantovani, A.; Sandrini, P. L.; Pertici, P.; Vitulli, G. *J. Organomet. Chem.* **1977**, *135*, 215.

(6) (a) Pertici, P.; Vitulli, G. *J. Chem. Soc., Dalton Trans.* **1983**, 1553. (b) Chaudret, B.; Commenges, G.; Poilblanc, R. *J. Chem. Soc., Chem. Commun.* **1982**, 1388. (c) Chaudret, B.; Commenges, G.; Poilblanc, R. *J. Chem. Soc., Dalton Trans.* **1984**, 1635.

(7) Hirano, M.; Marumo, T.; Miyasaka, T.; Fukuoka, A.; Komiya, S. *Chem. Lett.* **1997**, 291.

10.1021/om991014k CCC: $19.00
Publication on Web 08/25/2000

Scheme 1

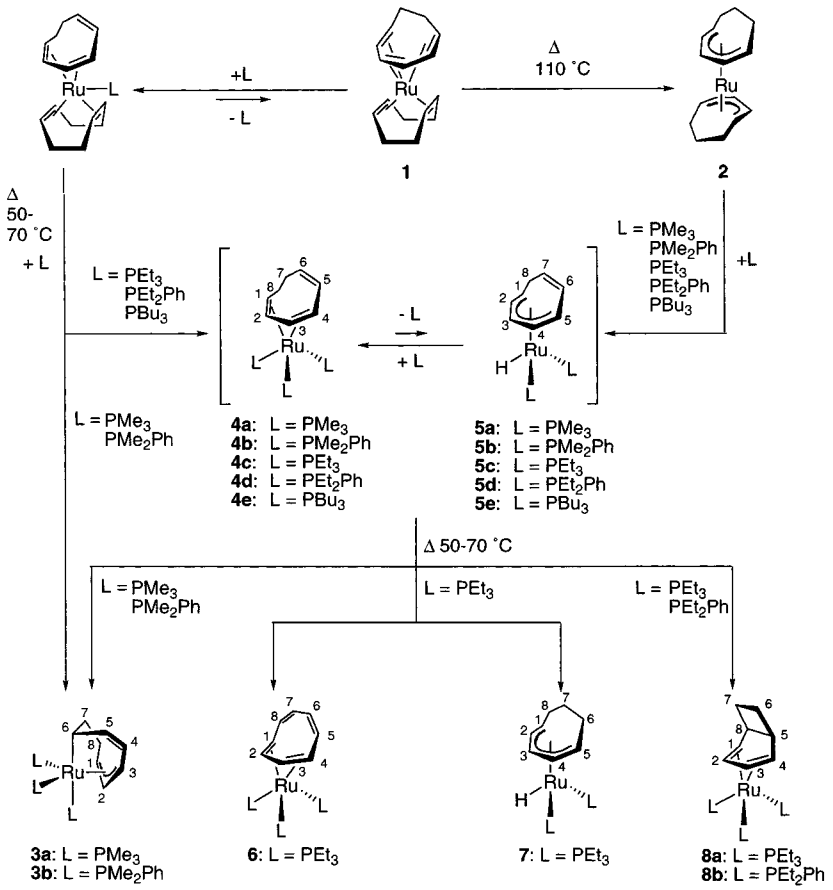

The $^{31}P\{^1H\}$ NMR spectrum of **3b** displays an ABX spin system, consistent with the absence of a symmetry plane in the complex at δ −1.9 (t, J = 24 Hz), 8.9 (dd, J = 22, 9 Hz), and 11.0 (dd, J = 24, 9 Hz) for the apical and two equatorial P nuclei, respectively. The ^1H NMR spectrum for **3b** shows two resonances at δ 5.71 (5-H) and 5.93 (4-H) for the uncoordinated olefinic protons of the cyclooctatriene ligand (see Scheme 1 for nomenclature). Resonances for the olefinic protons of the allyl moiety appear at δ 3.39 (3-H), 3.70 (1-H), and 4.05 (2-H), whereas the aliphatic protons exhibit a multiplet at δ 0.6−2.3. In addition, the IR spectrum for **3b** shows a band at 1634 cm^{-1} for the uncoordinated olefin. The NMR data for **3b** is in agreement with that of the related Ru(6-η^1:1−3-η^3-C_8H_{10})(PMe_3)$_3$ (**3a**).[7] The molecular structure for **3b** has been solved by X-ray structure analysis, as shown in Figure 1; crystallographic and data collection parameters are summarized in Table 1, and the bond distances and angles are listed in Table 2. Complex **3b** displays an octahedral geometry similar to that of **3a**,[7] indicating a divalent d^6 ruthenium complex.

Contrary to the reaction starting from **1**, the reaction of **2** with PMe_3 at room temperature for 24 h showed formation of the zerovalent complex Ru(η^4-C_8H_{10})(PMe_3)$_3$ (**4a**) (vide infra) in 54% yield, evolving 1,3-cyclooctadiene with concomitant formation of the divalent complex **3a** in 10% yield. In this reaction, one of the η^5-C_8H_{11} ligands in **2** is deprotonated to give the η^4-C_8H_{10}, whereas another η^5-C_8H_{11} ligand acts as a hydrogen acceptor to form 1,3-cyclooctadiene. When PMe_2Ph was employed in this reaction, Ru(η^4-C_8H_{10})(PMe_2Ph)$_3$ (**4b**) was formed in 74% yield with concomitant formation of **3b** in 25% yield after 24 h at room temperature. It is interesting to note that complexes **4a**,**b** were not detected in the reaction of **1** with PMe_3 or PMe_2Ph by NMR spectroscopy.[8]

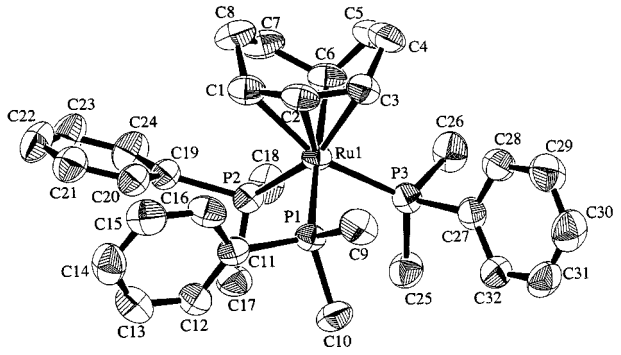

Figure 1. ORTEP drawing of **3b** showing 50% probability thermal ellipsoids. All hydrogen atoms are omitted for clarity.

(8) A possible explanation is that complexes **4a**,**b** are also intermediates in the formation of **3a**,**b** starting from **1** as well as that from **2**. However, while **4a**,**b** were not detected by the NMR in the formation of **3a**,**b** from **1**, conversion of **4a**,**b** to **3a**,**b** is slow enough to be observed by NMR spectroscopy under comparable conditions. Thus, as depicted in Scheme 1, formation of **3a**,**b** is likely to occur without formation of **4a**,**b** when the reaction was started from **1**.

(9) Bennett, M. A.; Matheson, T. W.; Robertson, G. B.; Smith, A. K.; Tucker, P. A. *Inorg. Chem.* **1981**, *20*, 2353, and references therein.

(10) Grassi, M.; Mann, B. E.; Manning, P.; Spencer, C. M. *J. Organomet. Chem.* **1986**, *307*, C55.

(11) Alibrandi, G.; Mann, B. E. *J. Chem. Soc., Dalton Trans.* **1992**, 1439.

(12) The equilibrium constant at the coalescence temperature.

Table 1. Crystallographic Data for 3b, 4c, 6, and 8b

	3b	4c	6	8b
formula	$C_{32}H_{43}P_3Ru$	$C_{26}H_{55}P_3Ru$	$C_{26}H_{53}P_3Ru$	$C_{38}H_{53}P_3Ru$
fw	621.68	561.71	559.70	703.83
cryst syst	triclinic	orthorhombic	monoclinic	triclinic
space group	$P\bar{1}$	*Iba*2	$P2_1/c$	$P\bar{1}$
a (Å)	11.143(2)	21.27(1)	16.995(5)	10.523(4)
b (Å)	14.934(2)	17.69(1)	9.45(2)	18.317(4)
c (Å)	9.254(2)	15.12(1)	18.188(6)	9.334(2)
α (deg)	94.49(1)			90.45(2)
β (deg)	91.32(2)		92.10(2)	99.55(2)
γ (deg)	83.02(1)			83.78(2)
V (Å^3)	1523.7(5)	5692(5)	2920(5)	1763.6(8)
Z	2	8	4	2
D_{calcd} (g cm^{-3})	1.355	1.311	1.273	1.325
temp (K)	293	113	293	293
μ (mm^{-1})	0.691	0.731	0.713	0.606
λ (Å)	0.7107	0.7107	0.7107	0.7107
no. collcd	7354	3407	6918	8568
no. obsd	4723	2763	2031	3960
refln/parameter ratio	14.53	10.20	7.49	10.45
R	0.0427	0.0458	0.0772	0.0463
R_w	0.0389	0.0497	0.0956	0.0522
GOF	2.195	2.20	1.874	0.826

Table 2. Selected Bond Lengths (Å) and Angles (deg) for Ru(6-η^1:1-3-η^3-C_8H_{10})(PMe_2Ph)$_3$ (3b)

Ru(1)−P(1)	2.375(1)	Ru(1)−P(2)	2.309(1)
Ru(1)−P(3)	2.318(1)	Ru(1)−C(1)	2.268(5)
Ru(1)−C(2)	2.176(4)	Ru(1)−C(3)	2.255(5)
Ru(1)−C(6)	2.214(5)	C(1)−C(2)	1.416(7)
C(1)−C(8)	1.537(7)	C(2)−C(3)	1.399(7)
C(3)−C(4)	1.491(7)	C(4)−C(5)	1.320(7)
C(5)−C(6)	1.485(7)	C(6)−C(7)	1.553(7)
C(7)−C(8)	1.507(7)		
P(1)−Ru(1)−P(2)	97.42(5)	P(1)−Ru(1)−P(3)	92.00(5)
P(1)−Ru(1)−C(1)	100.0(1)	P(1)−Ru(1)−C(2)	84.4(1)
P(1)−Ru(1)−C(3)	96.1(1)	P(1)−Ru(1)−C(6)	174.3(1)
P(2)−Ru(1)−P(3)	96.72(5)	P(2)−Ru(1)−C(1)	95.6(1)
P(2)−Ru(1)−C(2)	131.2(1)	P(2)−Ru(1)−C(3)	160.4(1)
P(2)−Ru(1)−C(6)	88.2(1)	P(3)−Ru(1)−C(1)	161.5(1)
P(3)−Ru(1)−C(2)	132.1(1)	P(3)−Ru(1)−C(3)	96.9(1)
P(3)−Ru(1)−C(6)	88.6(2)		

(b) PEt_3, PEt_2Ph, P(n-Bu)$_3$. Reactions of **1** with 3 equiv of these tertiary phosphines at 50 °C for 20 h in benzene or toluene afforded the zerovalent ruthenium complexes Ru(η^4-C_8H_{10})L_3 [L = PEt_3 (**4c**), PEt_2Ph (**4d**), P(n-Bu)$_3$ (**4e**)] in 43, 50, and 93% yields, respectively (Scheme 1). Complex **4c** was crystallized from hexane to afford orange crystals, suitable for X-ray structure analysis. The molecular structure of **4c** was determined by X-ray structure analysis (Figure 2). Crystallographic and data collection parameters are included in Table 1, and the bond distances and angles are listed in Table 3.

The molecular structure shows that the C_8H_{10} ligand coordinates in 1−4-η^4 fashion similar to Ru(η^4-C_8H_{10})-(η^4-C_8H_{12})[P(OMe)$_3$].[6a]

Complexes **4c**−**e** were characterized spectroscopically, on the basis of ^{1}H, ^{31}P, and ^{13}C NMR specta, ^{13}C{^{1}H} DEPT experiment, and ^{1}H−^{1}H, ^{1}H−^{31}P, and ^{1}H−^{13}C correlation experiments. For example, the ^{31}P{^{1}H} NMR spectrum of **4c** displays an AMX spin system at δ 14.7 (dd, J = 25, 6 Hz), 17.5 (dd, J = 25, 11 Hz), and 24.6 (dd, J = 11, 6 Hz) for two basal and the apical P nuclei, respectively, consistent with the absence of a symmetry plane in **4c**. The ^{1}H NMR spectrum shows two resonances at δ 6.22 and 5.32 for the uncoordinated olefinic protons of the C_8H_{10} ligand. Resonances for the olefinic protons coordinated to ruthenium appear at δ 4.74 (2H), 2.57 (1H), and 2.43 (1H). Accordingly, ^{13}C{^{1}H} NMR spectrum shows that all carbon atoms of the C_8H_{10} moiety are different (Table 4). Surprisingly, uncoordinated olefinic carbon atoms 5-C and 6-C display a small coupling with the phosphorus nuclei (4−8 Hz). This indicates that in solution there is a small contribution of a ruthenabicyclic structure as shown in structure I (**B**) and Table 4. This is further suggested by the fact that 2-C and 3-C for the related Ru(η^4-C_8H_{10})L_3 (**4c**−**e**) (vide infra) resonate as singlets in their ^{13}C{^{1}H} NMR spectra (Table 4). The absence of CP coupling in these two carbon atoms also suggests that the ruthenium center interacts more effectively with the C_5═C_6 double bond than with C_2═C_3 in this form (**B**) in solution; this coordination mode can explain the observed small J_{C_5P} (4−8 Hz) and J_{C_6P} (5−7 Hz) coupling constants (Table 4). Therefore, complex **4c** is considered to be a zerovalent ruthenium complex, with a small contribution of the ruthenabicyclic structure (**B**). Effective π-back-donation from the ruthenium center to the cyclooctatriene ligand is expected due to the highly reduced character of the ruthenium having three fairly basic phosphines. Thus, observation of such a ruthenabicyclic structure might be a reflection of this effective π-back-

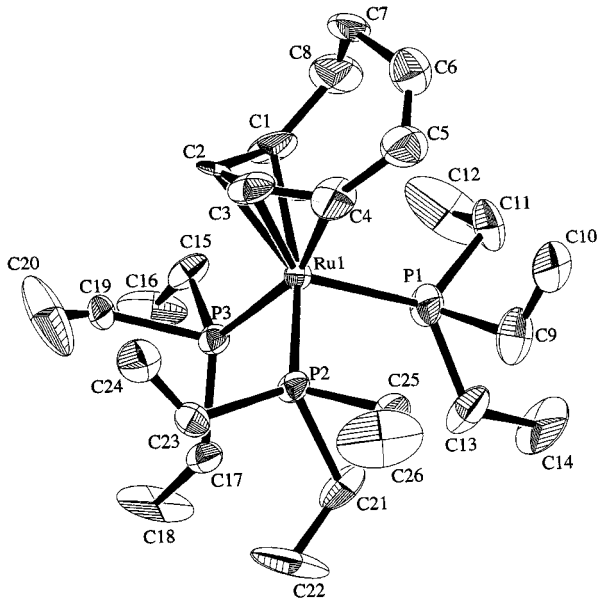

Figure 2. ORTEP drawing of **4c** showing 50% probability thermal ellipsoids. All hydrogen atoms are omitted for clarity.

Table 3. Selected Bond Lengths (Å) and Angles (deg) for Ru(η^4-C_8H_{10})(PEt_3)$_3$ (4c)

Ru(1)−P(1)	2.313(2)	Ru(1)−P(2)	2.343(5)
Ru(1)−P(3)	2.341(5)	Ru(1)−C(1)	2.33(1)
Ru(1)−C(2)	2.20(2)	Ru(1)−C(3)	2.16(2)
Ru(1)−C(4)	2.15(2)	C(1)−C(2)	1.53(2)
C(1)−C(8)	1.56(2)	C(2)−C(3)	1.40(1)
C(3)−C(4)	1.33(3)	C(4)−C(5)	1.43(2)
C(5)−C(6)	1.29(2)	C(6)−C(7)	1.52(2)
C(7)−C(8)	1.54(3)		
P(1)−Ru(1)−P(2)	98.3(2)	P(1)−Ru(1)−P(3)	96.7(2)
P(1)−Ru(1)−C(1)	99.2(5)	P(1)−Ru(1)−C(2)	137.1(5)
P(1)−Ru(1)−C(3)	135.8(6)	P(1)−Ru(1)−C(4)	102.0(6)
P(2)−Ru(1)−P(3)	94.83(7)	P(2)−Ru(1)−C(1)	160.8(5)
P(2)−Ru(1)−C(2)	121.8(5)	P(2)−Ru(1)−C(3)	93.9(5)
P(2)−Ru(1)−C(4)	88.4(7)	P(3)−Ru(1)−C(1)	91.0(6)
P(3)−Ru(1−C(2)	94.3(5)	P(3)−Ru(1)−C(3)	124.4(6)

Table 4. ^{13}C NMR Spectra of Cyclooctatriene Complexes Ru(η^4-C_8H_{10})L_3 (4)[a]

L	C(1)	C(2) and C(3)	C(4)	C(5)	C(6)	C(7)	C(8)
PEt_3	35.8 (dt) J_{CP} = 39, 4 Hz (J_{CH} = 137 Hz)	78.7−78.5 (m) (J_{CH} = 158 Hz)	43.0 (dt) J_{CP} = 32, 4 Hz (J_{CH} = 137 Hz)	138.6 (dd) J_{CP} = 8, 4 Hz (J_{CH} = 140 Hz)	115.3 (d) J_{CP} = 7 Hz (J_{CH} = 150 Hz)	27.5 (s)	24.7 (s)
PEt_2Ph	37.4 (dt) J_{CP} = 39, 4 Hz	79.6 (s), 81.1 (s)	43.2 (d) J_{CP} = 29 Hz	138.7 (brs)	116.1 (brd) J_{CP} = 5 Hz	27.6 (s)	21.0 (s)
P(n-Bu)$_3$	36.6 (dt) J_{CP} = 39, 4 Hz	78.6 (s), 79.6 (s)	43.2 (brd) J_{CP} = 31 Hz	138.9 (brs)	115.3 (d) J_{CP} = 5 Hz		21.0 (s)

[a] Chemical shifts measured in C_6D_6 at 25 °C (75.45 MHz). Abbreviations: s = singlet; m = multiplet; dt, double triplet; br, broad. Carbon atoms numbered as in Structure 1:

Structure 1

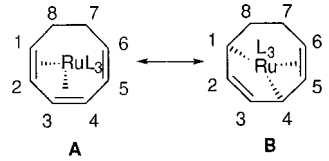

donation. NMR data for the related complexes **4d**,**e** is in agreement with that for **4c**, indicating also the existence in solution of the ruthenabicyclic structure (**B**).

The zerovalent ruthenium complexes Ru(η^4-C_8H_{10})-L_3 (**4c**−**e**) were also prepared by the reaction of the divalent complex **2** with the appropriate phosphines as shown in Scheme 1. Formation of **4c**−**e** was also accompanied by liberation of 1,3-cyclooctadiene, which is consistent with an intramolecular hydrogen transfer between cyclooctadienyl ligands in **2**.

Detailed analysis of the $^{31}P\{^1H\}$ NMR of **4c** in C_6D_6 or $C_6D_5CD_3$ at 25 °C revealed the existence of two other broad resonances at δ 30.5 and 34.8 as well as free PEt_3, together with the resonances for **4c**. The ^1H NMR spectrum also shows a broad triplet at δ −14.37, which seems to correspond with the two broad resonances in the $^{31}P\{^1H\}$ NMR. Interestingly, the resonance for the free PEt_3 in the $^{31}P\{^1H\}$ NMR also shows some broadening at room temperature ($\omega_{1/2}$ = 45 Hz), suggesting that phosphine dissociation is taking place in solution to afford the (hydrido)ruthenium(II) complex RuH(η^5-C_8H_9)(PEt_3)$_2$ (**5c**) (**4c**:**5c** = 8:1 ratio at 25 °C) according to Scheme 1. Cooling a sample of **4c** in $C_6D_5CD_3$ to −50 °C shows sharpening of the free PEt_3, and both broad resonances give rise to an AB quartet at δ 30.0 (d, J = 15 Hz) and 34.4(d, J = 15 Hz) for **5c**, without any change in the ratio of signals. At the same temperature, the broad triplet at δ −14.37 in the ^1H NMR spectrum also sharpened, giving a sharp triplet (J = 26.9 Hz). On further cooling to −70 °C, at least three other minor species were observed (see Experimental Section). On the other hand, the dissociation process is enhanced on warming a sample containing a mixture of **4c** and **5c**, the latter one being the only species observed at 90 °C. Further evidence for the dissociation process was obtained by addition of 4 equiv of PEt_3, which shifted the equilibrium completely to **4c**. Complexes **4d**,**e** show similar dissociation processes, affording the corresponding hydridoruthenium(II) complexes **5d**,**e**, as shown in Scheme 1. Unlike complexes **5c** and **5e**, complex **5d** is the major species in solution (**4d**:**5d** = 1:3 ratio at 25 °C). Thus, the cyclooctatrienyl protons in complex **5d** could be fully assigned by a combination of low-temperature $^1H-^1H$ COSY and homo-decoupling experiments as well as by comparison with the spectra of related cyclic η^5-C_8H_9 complexes.[9] Thus, the triplet resonance in the ^1H NMR of **5d** at δ 4.67 is assigned to the central allylic 3-H (see Scheme 1 for numbering), which is coupled to the two adjacent protons 2- and 4-H ($J_{H_3H_4} = J_{H_2H_3}$ = 7.5 Hz). Then, decoupling experiments at −20 °C established connectivity permitting the assignment of the rest of the cyclooctatrienyl ligand. The uncoordinated protons 7- and 6-H display a doublet (J = 6.8 Hz) and a double triplet (J = 6.8, 4.5 Hz) at δ 5.43 and 5.75, respectively. The rest of resonances appear as multiplets at δ 3.95 (1-H), 3.7 (5-H), 3.65 (4-H), and 3.00 (2-H). The methylene protons (8-CH_2) are obscured by the depe signals. Assignment of the cyclooctatrienyl moiety in complexes **5c** and **5e** was also made by a combination of low-temperature ^1H and $^{31}P\{^1H\}$ NMR experiments and by comparison with **5d**.

It is noteworthy that the two broad resonances observed in the $^{31}P\{^1H\}$ NMR spectra of **5c**−**e** at 25 °C coalesce into a single broad resonance at higher temperatures. Thus, the two broad resonances at δ 30.5 and 34.8 for **5c** coalesce into a broad resonance at δ 35.2 (T_C = 323 K) in the $^{31}P\{^1H\}$ NMR spectrum. Such dynamic behavior is likely due to rotation of the RuH-(PEt_3)$_2$ moiety with respect to the η^5-C_8H_9. A similar mechanism has been established for the related chloro complexes RuCl(η^5-C_7H_9)(PPh_3)$_2$[10] and RuCl(η^5-C_8H_9)-(PPh_3)$_2$.[11] An activation energy $\Delta G^‡$ of 14.4 kcal/mol was calculated for this exchange process at the coalescence temperature (T_C = 323 K) in **5c** and for a K of 1160 s^{-1}.[12] Similarly, an activation energy $\Delta G^‡$ of 14.7 kcal/mol was calculated for complex **5e**. The activation energy for RuCl(η^5-C_8H_9)(PPh_3)$_2$ was reported to be 14.7 kcal/mol.[11] The latter complex is known to give a mixture of three isomers in solution. Two of those were characterized as rotamers of RuCl(η^5-C_8H_9)(PPh_3)$_2$ by rotation of the RuCl(PPh_3)$_2$ moiety, and the third one was characterized as {2,3,4,5,6-η^5-bicyclo[5.1.0]octadienyl}chlorobis(triphenylphosphine)ruthenium(II). This is consistent with the observation of at least two other small isomers for **5c**−**e** at low temperature in our case. However, the low concentration of these species in solution prevented full characterization. Formation of **5a**,**b** from **4a**,**b** was negligible probably because the equilibrium lies so far toward **4a**,**b**.

Thermal Isomerization of Ru(η^4-C_8H_{10})L_3 (4). (a) PMe_3, PMe_3Ph. As described above, heating of the complexes **4a** and **4b** led to **3a** and **3b**, respectively, where the η^4-C_8H_{10} fragment oxidatively adds to the ruthenium(0) center giving the η^1:η^3-C_8H_{10} ligand.

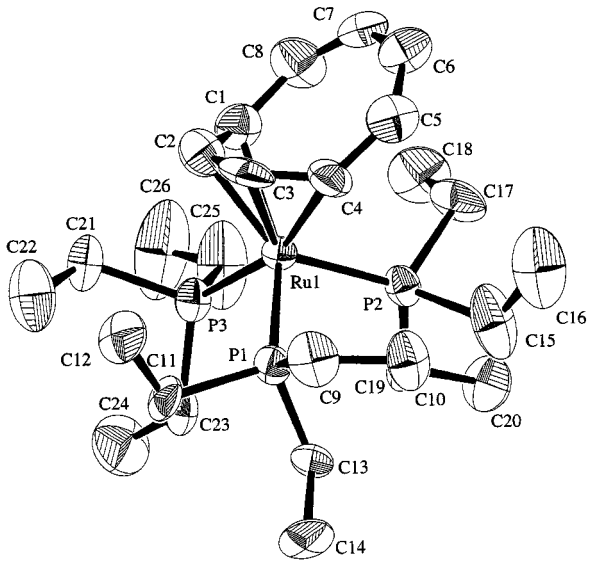

Figure 3. ORTEP drawing of **6** showing 50% probability thermal ellipsoids. All hydrogen atoms are omitted for clarity.

Table 5. Selected Bond Lengths (Å) and Angles (deg) for Ru(η^4-C_8H_8)(PEt_3)$_3$ (6)

Ru(1)−P(1)	2.326(5)	Ru(1)−P(2)	2.344(6)
Ru(1)−P(3)	2.345(6)	Ru(1)−C(1)	2.33(2)
Ru(1)−C(2)	2.13(2)	Ru(1)−C(3)	2.17(2)
Ru(1)−C(4)	2.33(2)	C(1)−C(2)	1.44(3)
C(1)−C(8)	1.47(3)	C(2)−C(3)	1.41(3)
C(3)−C(4)	1.36(3)	C(4)−C(5)	1.43(3)
C(5)−C(6)	1.41(3)	C(6)−C(7)	1.41(3)
C(7)−C(8)	1.37(3)		
P(1)−Ru(1)−P(2)	97.2(2)	P(1)−Ru(1)−P(3)	97.3(2)
P(1)−Ru(1)−C(1)	154.9(6)	P(1)−Ru(1)−C(2)	117.9(6)
P(1)−Ru(1)−C(3)	92.4(6)	P(1)−Ru(1)−C(4)	90.1(6)
P(2)−Ru(1)−P(3)	96.5(2)	P(2)−Ru(1)−C(1)	107.7(6)
P(2)−Ru(1)−C(2)	141.7(6)	P(2)−Ru(1)−C(3)	133.3(7)
P(2)−Ru(1)−C(4)	99.2(6)	P(3)−Ru(1)−C(1)	83.8(6)
P(3)−Ru(1)−C(2)	93.8(7)	P(3)−Ru(1)−C(3)	127.4(7)
P(3)−Ru(1)−C(4)	161.7(6)		

(b) PEt_3. On the other hand, prolonged heating of the isolated **4c** in benzene at 70 °C for 100 h caused disproportionation reaction of the η^4-C_8H_{10} moiety to give a mixture of Ru(η^4-C_8H_8)(PEt_3)$_3$ (**6**) and RuH(η^5-C_8H_{11})(PEt_3)$_3$ (**7**) in 43 and 42% yields, respectively. The reaction of **2** with 4 equiv of PEt_3 at 50 °C for 3 days also gave **6** and **7** in 1:1 ratio, from which complex **6** was preferentially given in 13% yield. The solid structure of complex **6** was confirmed by a single-crystal X-ray structure analysis. An ORTEP drawing of the molecule is shown in Figure 3; crystallographic data collection parameters are included in Table 1, and bond distances and angles are provided in Table 5.

The bond angles P1−Ru1−P2 [97.2(2)°], P1−Ru1−P3 [97.3(2)°], and P2−Ru1−P3 [96.5(2)°] are consistent with a distorted square-pyramidal structure with P2 in the apical position and P1 and P3 in the basal positions. The other two basal positions are occupied by the C1−C2 and C3−C4 bonds. The mean metal−carbon bond lengths to the inner carbon atoms [2.15(2) Å for Ru1−C2 and Ru1−C3] are significantly shorter than that to the outer carbon atoms [2.33(2) Å for Ru1−C1 and Ru1−C4], indicating that the C_8H_8 ligand is also coordinating in an η^4-fashion. The inner metal−carbon bond lengths are longer than that in Ru(η^4-C_8H_8)(η^6-HMB) [2.120-(10), 2.233(10) Å][13] but shorter than that in the related Ru(η^4-C_8H_8)$(CO)_3$ [2.182(6), 2.265(6) Å].[14] The outer bond lengths are similar to those in Ru(η^4-C_8H_8)$(CO)_3$. The dihedral angle between the coordinated and uncoordinated diene sections is 42(1)° in **6** [cf. Ru(η^4-C_8H_8)(η^6-HMB), 45.4°; Ru(η^4-C_8H_8)$(CO)_3$, 42.5°]. The C−C distances for the C_8H_8 ring in **6** are very similar [1.36(3)−1.44(3) Å] (Table 5). Such a trend was found in Ru(η^4-C_8H_8)(η^6-HMB), though less marked in Ru(η^4-C_8H_8)$(CO)_3$. As Bennett[13] already suggested for the later complexes, the equality in bond lengths is probably due to electron delocalization over the entire C_8H_8 ring. He proposed that increasing the back-bonding to the C_8H_8 in M(arene)(η^4-C_8H_8) relative to Ru(η^4-C_8H_8)$(CO)_3$ might cause the eight-membered ring to approach more closely the aromatic system $(C_8H_8)^{2-}$. Our complex nicely fits this scenario since the PEt_3 ligands increase the electron density on the ruthenium center and consequently increase the back-bonding to the C_8H_8 ligand.

The $^{31}P\{^1H\}$ NMR spectrum for **6** displays a singlet at δ 27.7, suggesting that the complex does not keep its solid structure in solution and the ruthenium center is migrating around the C_8H_8 ring. A unique singlet for all protons of the cyclooctatetraene ring in the ^1H NMR spectrum for **6** at δ 5.22 confirmed that the migration process occurs at 23 °C. These data are consistent with a sequence of 1,2-shifts of the metal with its cyclooctatetraene ligand, similarly to the related Ru(η^4-C_8H_8)(η^6-HMB) and M(η^4-C_8H_8)$(CO)_3$ (M = Fe, Ru, Os).[13,14] The C_8H_8 singlet in the ^1H NMR spectrum for **6** broadens at about −40 °C and collapses into the baseline at −80 °C. Similarly, the singlet in the $^{31}P\{^1H\}$ NMR spectrum for **6** also broadens at about −80 °C.

In situ NMR studies of the disproportionation reaction of **4c** revealed the formation of the (hydrido)ruthenium complex RuH(η^5-C_8H_{11})(PEt_3)$_3$ (**7**) together with **6**. However, only complex **6** could be crystallized from the mixture, probably due to its lower solubility. Thus, complex **7** was characterized spectroscopically. The ^1H NMR spectrum for **7** displays a triplet resonance at δ −11.6 (J = 31 Hz) for the Ru-*H* due to coupling with two inequivalent P nuclei. The cyclooctadienyl protons appear as broad resonances, typical of η^5-cyclooctadienyl ligands at δ 2.49 (1- and 5-H), 3.45 (3-H), and 4.85 (2- and 4-H).[15]

Whereas prolonged heating of the isolated **4c** at 70 °C for 4 days resulted in the disproportionation reaction giving **6** and **7**, the prolonged reaction of **1** with 3 equiv of PEt_3 under comparable conditions produced a bicyclic complex Ru(η^4-bicyclo[4.2.0]octa-2,4-diene)(PEt_3)$_3$ (**8a**) in 38% yield via **4c**. Detailed analysis of this reaction showed no interconversion among complexes **6**, **7**, and **8a**. One possible explanation for this is the difference of the concentration of **4c** because the disproportionation reaction giving **6** and **7** would be regarded as a bimolecular reaction, while the formation of **8a** is likely due to an intramolecular reaction. In fact, it was found that regardless of the concentration, heating of the isolated **4c** finally gave **6** and **7**. Another possibility considered is that the liberated 1,5-cyclooctadiene from **1** could

(13) Bennett, M. A.; Matheson, T. W.; Robertson, G. B.; Smith, A. K.; Tucker, P. A. *Inorg. Chem.* **1980**, *19*, 1014, and references therein.
(14) Cotton, F. A.; Eiss, R. *J. Am. Chem. Soc.* **1969**, *91*, 6593.
(15) Bouachir, F.; Chaudret, B.; Dahan, F.; Agbossou, F.; Tkatchenko, I. *Organometallics* **1991**, *10*, 455.

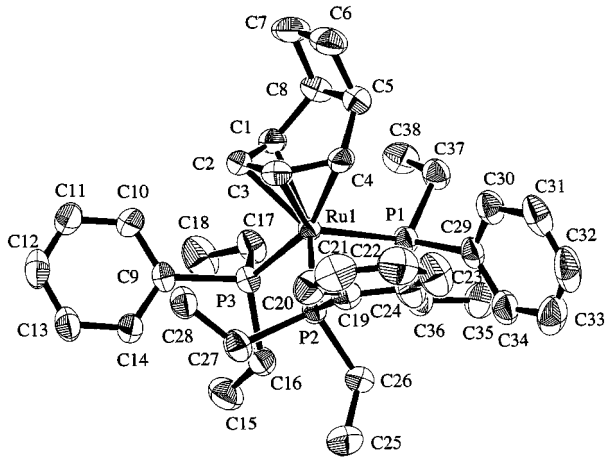

Figure 4. ORTEP drawing of **8b** showing 50% probability thermal ellipsoids. All hydrogen atoms are omitted for clarity.

Table 6. Selected Bond Lengths (Å) and Angles (deg) for Ru(η^4-bicyclo[4.2.0]octa-2,4-diene)-(PEt_2Ph)$_3$ (8b)

Ru(1)−P(1)	2.338(2)	Ru(1)−P(2)	2.320(2)
Ru(1)−P(3)	2.350(2)	Ru(1)−C(1)	2.230(7)
Ru(1)−C(2)	2.158(7)	Ru(1)−C(3)	2.155(7)
Ru(1)−C(4)	2.245(7)	C(1)−C(2)	1.447(10)
C(1)−C(8)	1.506(9)	C(2)−C(3)	1.414(9)
C(3)−C(4)	1.431(9)	C(4)−C(5)	1.520(10)
C(5)−C(6)	1.55(1)	C(5)−C(8)	1.56(1)
C(6)−C(7)	1.53(1)	C(7)−C(8)	1.54(1)
P(1)−Ru(1)−P(2)	99.40(6)	P(1)−Ru(1)−P(3)	98.72(7)
P(1)−Ru(1)−C(1)	105.7(2)	P(1)−Ru(1)−C(2)	142.0(2)
P(1)−Ru(1)−C(3)	133.1(2)	P(1)−Ru(1)−C(4)	95.2(2)
P(2)−Ru(1)−P(3)	94.55(7)	P(2)−Ru(1)−C(1)	153.2(2)
P(2)−Ru(1)−C(2)	114.8(2)	P(2)−Ru(1)−C(3)	89.2(2)
P(2)−Ru(1)−C(4)	96.3(2)	P(3)−Ru(1)−C(1)	91.0(2)
P(3)−Ru(1)−C(2)	94.8(2)	P(3)−Ru(1)−C(3)	126.7(2)
P(3)−Ru(1)−C(4)	160.7(2)		

change the final product distribution. Addition of 1 equiv of 1,5-cyclooctadiene to **4c** led to the final product of **8a**. The origin of effect of 1,5-cyclooctadiene is unclear.

(c) PEt_2Ph. When the diethylphenylphosphine complex **4d** was heated to 70 °C for 4 days in benzene, the cyclooctatriene ligand isomerized to the bicyclo[4.2.0]-octa-2,4-diene at ruthenium to give **8b**. The molecular structure of **8b** was confirmed by X-ray structure analysis (Figure 4). Crystal and data collection parameters are included in Table 1, and selected bond distances and angles are shown in Table 6.

Although such intramolecular cyclizations of cyclooctatriene are documented for free cyclooctatriene,[16] the coordinated cyclooctatriene at the $Ru(CO)_3$ fragment,[17] the reaction of $RuCl_3$ with cyclooctatriene,[18] and the reaction of **1** giving Ru(η^4-bicyclo[4.2.0]octa-2,4-diene)-(μ-CO)(μ_3-CO)$Rh_2Cp^*_2$,[19] it is important to note that in our case complexes with PEt_3 and PEt_2Ph favor such an isomerization. The molecular structure of **8b** is also consistent with a distorted square-pyramidal structure with P1 in the apical position and P2 and P3, C1−C2, and C3−C4 bonds in the basal positions. The Ru−C bond distances Ru1−C1 [2.230(1) Å], Ru1−C2 [2.158-(2) Å], Ru1−C3 [2.155(2) Å], and Ru1−C4 [2.245(2) Å] show an η^4-coordination mode of the diene moiety to ruthenium as in the previous cases, complexes **4c** and **6**.

Scheme 2

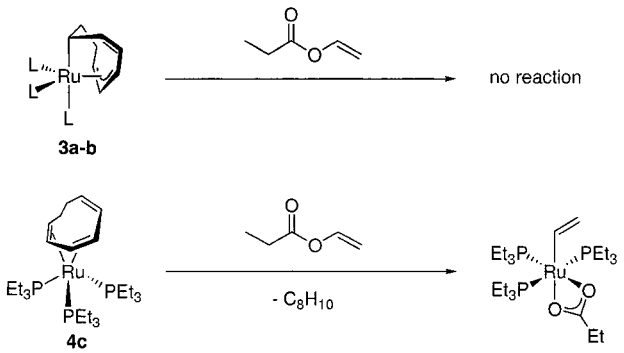

The ^{1}H NMR spectrum for **8b** shows six multiplets for the bicyclo-C_8H_{10} moiety at δ 1.59 (2H, *endo*-6- and 7-H), 2.08 (1H, *exo*-6- or 7-H), 2.09 (1H, *exo*-7- or 6-H), 2.37 (2H, 1- and 4-H), 2.57 (2H, 5- and 8-H), and 4.60 (2H, 2- and 3-H), in agreement with the X-ray structure and consistent with the related complex Ru(bicyclo-C_8H_{10})$(CO)_3$.[17] The ^{31}P{^{1}H} NMR spectrum for complex **8b** displays two broad resonances at δ 26.9 and 36.2 in 2:1 ratio at 25 °C, probably due to the rotation of the $Ru(PEt_2Ph)_3$ moiety with respect to the bicyclo-C_8H_{10} ligand in **8b**.

C−O Bond Cleavage of Vinyl Propionate by Ruthenium. An interesting feature of the (η^4-cyclooctatriene)ruthenium(0) complex **4c** is its high reactivity toward the C−O bond oxidative addition of vinyl propionate giving (η^1-vinyl)(carboxylato)ruthenium(II) complex,[20] whereas a similar reaction of **3a**,**b** did not take place at all (Scheme 2). These present results are of special relevance in the ruthenium-promoted C−O bond cleavage reactions.[20−22] Whereas the cyclooctatriene ligand in the zerovalent complex **4c** can be displaced by the vinylic substrate affording eventually the oxidative addition product Ru(η^1-C_2H_3)(OCOEt)$(PEt_3)_3$, the η^1:η^3-C_8H_{10} ligand in the divalent complexes **3a**,**b** is strongly bonded to ruthenium so that neither displacement reaction nor oxidative addition of the vinyl-oxygen bond is observed.

Concluding Remarks. The observation of these various coordination modes of the C_8H_{10} ligand at Ru can be rationalized as follows: the reaction of **1** with tertiary phosphine ligands initially gives the known phosphine adduct Ru(η^4-C_8H_{12})(η^4-C_8H_{10})(L),[6,7] although sterically demanding ligands such as P^iPr_3, PCy_3, and PPh_3 remain unreacted. Further displacement of the η^4-C_8H_{12} ligand in Ru(η^4-C_8H_{12})(η^4-C_8H_{10})(L) by tertiary

(16) Adam, W.; Gretzke, N.; Hasemann, L.; Klug, G.; Peters, E.-M.; Peters, K.; von Schmering, H. G.; Will, B. *Chem. Ber.* **1985**, *118*, 3357.
(17) Johnson, B. F. G.; Domingos, A. J. P.; Lewis, J. *J. Organomet. Chem.* **1973**, *49*, C33.
(18) Müller, J.; Fischer, E. O. *J. Organomet. Chem.* **1966**, *5*, 275.
(19) Farrugia, L. J.; Jeffery, J. C.; Marsden, C.; Stone, F. G. A. *J. Chem. Soc., Dalton Trans.* **1985**, 645.
(20) Komiya, S.; Suzuki, J.; Miki, K.; Kasai, M. *Chem. Lett.* **1987**, 1287.
(21) (a) Hirano, M.; Kurata, N.; Marumo, T.; Komiya, S. *Organometallics* **1998**, *17*, 501. (b) Komiya, S.; Kabasawa, T.; Yamashita, K.; Hirano, M.; Fukuoka, A. *J. Organomet. Chem.* **1994**, *471*, C6. (c) Planas, J. G.; Hirano, M.; Komiya, S. *Chem. Lett.* **1998**, 123. (d) Planas, J. G.; Marumo, T.; Ichikawa, Y.; Hirano, M.; Komiya, S. *J. Mol. Catal.* **1999**, *147*, 137.
(22) Further studies concerning the relationship between the structure and the reactivities toward C−O bond cleavage will be described elsewhere.

phosphine ligand gives the η^1:η^3-C_8H_{10} complexes **3a**,**b** or η^4-C_8H_{10} complexes **4c**−**e**. The same complexes can also be obtained by the reaction of **2** with the appropriate phosphines, by intramolecular hydrogen transfer between the cyclooctadientyl ligands in **2**, affording **4c**−**e** and 1,3-cyclooctadiene. Complexes **4a**,**b** are formed only when **2** is employed as a starting complex. These data clearly demonstrate that whereas phosphine ligands with small cone angles (ca. 100−120°) preferentially form the divalent Ru(η^1:η^3-C_8H_{10})L_3 (**3a**,**b**) as thermodynamically stable complexes, phosphine ligands with a slightly larger cone angle (ca. 130°) were found to give preferentially the zerovalent Ru(η^4-C_8H_{10})L_3 (**4**), with phosphine ligands with larger cone angles not reacting.[23] The fact that PCy_3, which has electron-donating properties comparable with PEt_3 or P(n-Bu_3), did not react suggests that the size of the phosphine ligand is the most important factor in determining the final products. Stabilization of the η^1:η^3-C_8H_{10} coordination mode in the case of more compact phosphine ligands such as PMe_3 or PMe_2Ph might be due to a weaker steric repulsion among the C_8H_{10} moiety and the three small phosphine ligands in **3a**,**b** than in the case of the bulkier PEt_3, P(n-Bu)$_3$, or PEt_2Ph ligands in **4c**−**e**. Selective displacement of the cyclooctadiene ligand in **1** by monodentate trialkylphosphines is surprising, since the small CO ligand was found to displace the cyclooctatriene ligand in **1**, selectively.[5] One possible explanation for this might be a more effective Ru-to-cyclooctatriene π-back-donation in our case than in the case of CO. Observation of the ruthenabicyclic structure (**B**) in solution supports this hypothesis. Although the ligand displacement reactions in **1** by monodentate trialkylphosphines seems to be controlled, mainly by steric factors, in a broader context including other ligands such as CO or arenes, electronic factors cannot be neglected.

In benzene solution, **4c**−**e** easily released a phosphine ligand, leading to the equilibrium mixture with **5c**−**e** at room temperature, probably because of the steric repulsion between ligands at Ru. The higher stabilization of the η^1:η^3-C_8H_{10} coordination mode in **3a**,**b** would discourage the dissociation of the phosphine ligand. For the PEt_3 complex **4c**, further disproportionation reaction giving **6** and **7** takes place, indicating occurrence of a facile intermolecular hydride transfer reaction. On the other hand, the prolonged heating of **4d**, having sterically more bulky PEt_2Ph ligands, gave the η^4-bicyclo[4.2.0]octa-2,4-diene complex **8b** by the intramolecular isomerization of the C_8H_{10} ligand.

Experimental Section

General Information. All reactions and manipulations were routinely performed under a dry nitrogen or argon atmosphere using Schlenk and vacuum-line techniques. Benzene, hexane, and toluene were dried over sodium benzophenone ketyl, distilled, and stored in gastight solvent bulbs. Benzene-d_6 and toluene-d_8 were dried over sodium metal and vacuum-distilled prior to use. All the trialkylphosphines were prepared by the reactions of $P(OPh)_3$ with the appropriate Grignard reagents. Ru(η^4-C_8H_{12})(η^6-C_8H_{10}) (**1**) and Ru(η^5-C_8H_{11})$_2$ (**2**) were prepared by the literature methods.[24] Vinyl propionate was purchased from Aldrich Chemical Co. and purified by distillation. Infrared spectra were measured on a JASCO FT/IR-410 spectrometer. ^{1}H, ^{1}H−^{1}H COSY, ^{31}P{^{1}H}, ^{13}C{^{1}H} NMR, DEPT, and ^{1}H−^{13}C correlation spectra were obtained on a JEOL LA-300 spectrometer. ^{1}H NMR chemical shifts are reported in ppm downfield of tetramethylsilane, using residual solvent resonances as internal standards. ^{31}P NMR chemical shifts are relative to an external standard, 85% H_3PO_4. Elemental analysis was performed with a Perkin-Elmer 2400 Series II CHNS analyzer.

Preparation of *fac*-[Ru(6-η^1:1−3-η^3-C_8H_{10})L_3] (3). [L = PMe_3]. As reported previsously,[7,21d] the reaction of **1** with PMe_3 gave **3a** with concomitant formation of 1,5-cyclooctadiene.

[L = PMe_2Ph]. PMe_2Ph (140.2 μL, 0.9967 mmol) was added to a solution of **1** (104.8 mg, 0.3322 mmol) in 5 mL of hexane, and the reaction mixture was stirred at 50 °C for 24 h. After removal of the volatile materials, the residual yellow oil was recrystallized from pentane/THF (2:1) to afford a pale yellow solid. The yellow solid was then washed with pentane, dried under vacuum, and recrystallized from benzene to yield **3b** as yellow crystals (51.2 mg, 0.0821 mmol): yield 25%. Anal. Calcd for $C_{32}H_{43}P_3Ru$: C, 61.82, H, 6.97. Found: C, 61.74; H, 7.25. IR (KBr, cm^{-1}): 1634m (νC═C). ^{1}H NMR (C_6D_6, rt, 300.4 MHz): δ 0.60 (d, J = 4.8 Hz, 3H, *eq*-PMe_2Ph), 0.93 (d, J = 6.3 Hz, 3H, *eq*-PMe_2Ph), 1.46 (d, J = 6.3 Hz, 3H, *eq*-PMe_2Ph), 1.67 (d, J = 6.3 Hz, 3H, *eq*-PMe_2Ph), 1.7 (1H, overlapped with PMe_2-Ph, 8-CH_2), 1.73 (d, J = 6.7 Hz, 6H, *ap*-PMe_2Ph), 2.0 (br, 1H, 6-C*H*), 2.1−2.3 (m, 3H, 7- and 8-CH_2), 3.39 (m, 1H, 3-C*H*═), 3.70 (m, 1H, 1-C*H*═), 4.05 (dt, J = 16.5, 10.4 Hz, 1H, 2-C*H*═), 5.71 (m, 1H, 5-C*H*═), 5.93 (m, 1H, 4-C*H*═), 7.0−7.7 (m, 15H, PMe_2*Ph*). ^{31}P{^{1}H} NMR (C_6D_6, rt, 121.6 MHz): δ −1.9 (t, J = 24 Hz, 1P, *ap*-PMe_2Ph), 8.9 (dd, J = 22, 9 Hz, 1P, *eq*-PMe_2-Ph), 11.0 (dd, J = 24, 9 Hz, 1P, *eq*-PMe_2Ph).

Preparation of Ru(η^4-C_8H_{10})L_3 (4). [L = PEt_3 (4c)]. Procedure A. A typical procedure for **4c** is given. Triethylphosphine (300 μl, 2.03 mmol) was added to a solution of **1** (159.3 mg, 0.5057 mmol) in 3 mL of toluene. The reaction mixture was stirred at 50 °C for 20 h. After volatile materials were removed, the residual orange oil was crystallized from hexane to give orange crystals, which were washed with pentane and dried under vacuum to yield **4c** (123.0 mg, 0.2190 mmol): yield 43%. Anal. Calcd for $C_{26}H_{55}P_3Ru$: C, 55.60; H, 9.87. Found: C, 56.08; H, 10.11. IR (KBr, cm^{-1}): 1636. ^{1}H NMR (300 MHz, C_6D_6): δ 0.87 (dt, J = 12.0, 6.1 Hz, 18H, PCH_2CH_3), 1.10 (dt, J = 12.0, 8.1 Hz, 9H, PCH_2CH_3), 1.3−1.4 (1H, 8-CH_2, overlapped with signals due to PEt_3), 1.31−1.58 (m, 12H, PCH_2CH_3), 1.88−2.05 (m, 6H, PCH_2CH_3), 1.90−2.00 (m, 1H, 8-CH_2), 2.01−2.19 (m, 1H, 7-CH_2), 2.39 (m, 1H, 7-CH_2), 2.43 (m, 1H, 4-C*H*═), 2.57 (m, 1H, 1-C*H*═), 4.74 (m, 2H, 2- and 3-C*H*═), 5.32 (m, 6-C*H*═), 6.22 (t, J = 9.2 Hz, 1H, 5-C*H*═). ^{31}P{^{1}H} NMR (121.6 MHz, rt, C_6D_6): δ 14.7 (dd, J = 25, 6 Hz, 1P), 17.5 (dd, J = 25, 11 Hz, 1P), 24.6 (dd, J = 11, 6 Hz, 1P). ^{13}C{^{1}H} NMR (74.5 MHz, rt, C_6D_6): δ 9.3(d, J = 3 Hz, PCH_2CH_3), 9.4 (d, J = 3 Hz, PCH_2CH_3), 10.0 (d, J = 4 Hz, PCH_2CH_3), 20.6 (s, 8-CH_2), 22.5 (d, J = 14 Hz, PCH_2CH_3), 22.9 (d, J = 14 Hz, PCH_2CH_3), 24.7 (d, J = 17 Hz, PCH_2CH_3), 27.5 (s, 7-CH_2), 35.8 (dt, J = 39, 4 Hz, 1-C*H*═), 43.0 (dt, J = 32, 4 Hz, 4-C*H*═), 78.5−78.7 (m, 2- and 3-C*H*═), 115.3 (d, J = 7 Hz, 6-C*H*═), 138.6 (dd, J = 8, 6 Hz, 5-C*H*═). **Procedure B.** A typical procedure for **4c** is given. Triethylphosphine (556 μl, 3.76 mmol) was added to a solution of **2** (289.6 mg, 0.9181 mmol) in 4 mL of toluene. The reaction mixture was stirred at 65 °C for 5 h. After volatile materials were removed, the residual orange oil was crystallized from hexane to give orange crystals for **4c** (219.2 mg, 0.3902 mmol): yield 43%.

(23) Cone angles for the tertiary phosphines are as follows: PMe_3 (118°), PMe_2Ph (122°), PEt_3 (132°), P^{n}Bu$_3$ (132°), PEt_2Ph (136°), PPh_3 (145°), P^{i}Pr (160°), and PCy_3 (170°): Tolman, C. A. *Chem. Rev.* **1977**, *77*, 313.

(24) (a) Pertici, P.; Vitulli, G. *J. Chem. Soc., Dalton Trans.* **1979**, 1961. (b) Itoh. K.; Nagashima, H.; Ohshima, T.; Oshima, N.; Nishiyama, H. *J. Organomet. Chem.* **1984**, *272*, 179.

The following complexes were prepared by procedure A except for **4a**,**b**. The amount of reactants used, yields, and analytical and spectroscopic data are summarized in Table 4 or below.

[L = PMe_3 (4a)]. Complex **2** (15.2 mg, 0.0482 mmol) was placed into an NMR tube, and then C_6D_6 (500 μL), PMe_3 (20 μL, 0.19 mmol), and PPh_3 as an internal standard were added. The NMR tube was mechanically stirred at room temperature, and the ^{1}H and $^{31}P\{^1H\}$ NMR specta were measured periodically. After 24 h, complex Ru(η^4-C_8H_{10})(PMe_3)$_3$ (**4a**) was formed in 54% yield with concomitant formation of **3a** in 10% yield. These yields did not vary during the following 150 h. Further reaction at 50 °C for an additional 96 h led to **4a** and **3a** in 4 and 84% yields, respectively. Complex **4a** was characterized spectroscopically in a mixture of **4a** and **3a**. Selected NMR data: ^{1}H NMR (300 MHz, C_6D_6): δ 4.51 (m, 2H, 2- and 3-C*H*═), 5.21 (m, 1H, 6-C*H*═), 6.23 (t, J = 9.0 Hz, 1H, 5-C*H*═), and other signals were obscured due to overlapping with **3a**. $^{31}P\{^1H\}$ NMR (121.5 MHz, C_6D_6): δ −3.7 (dd, J = 27, 8 Hz, 1P), 0.0 (dd, J = 11. 8 Hz, 1P),1.0 (dd, J = 27 11 Hz, 1P).

[L = PMe_2Ph (4b)]. Complex **2** (11.2 mg, 0.0355 mmol) was placed in an NMR tube, and C_6D_6 (500 μL) and PMe_2Ph (20 μL, 0.14 mmol) were introduced in this order. The NMR data show slow formation of Ru(η^4-C_8H_{10})(PMe_2Ph)$_3$ (**4b**) at room temperature for 24 h in 74% yield with concomitant formation of **3b** in 25% yield. Heating of the mixture at 50 °C for 24 h led to the formation of **3b** with the final distribution of **4b** and **3b** being 10 and 83% yield, respectively. Complex **4b** was characterized spectroscopically in a mixture of **4b** and **3b**. Selected NMR data: ^{1}H NMR (300.4 MHz, C_6D_6): δ 4.22−4.49 (m, 2H, 2- and 3-C*H*═), 5.12 (m, 1H, 6-C*H*═), 6.06 (t, J = 9.0 Hz, 1H, 5-C*H*═). $^{31}P\{^1H\}$ NMR (121.5 MHz, C_6D_6): δ 5.75 (dd, J = 25, 5 Hz, 1P), 9.9 (dd, J = 25, 7 Hz, 1P), 10.6 (dd, J = 7, 5 Hz, 1P).

[L = PEt_2Ph (4d)]. 1 (178.6 mg, 0.567 mmol), diethylphenylphosphine (395 μl, 2.27 mmol), and **4d** (199.4 mg, 0.283 mmol) were used: yield 50%. Anal. Calcd for $C_{38}H_{55}P_3Ru$: C, 64.66; H, 7.85. Found: C, 64.34; H, 8.06. IR (KBr, cm^{-1}): 1636. ^{1}H NMR (300 MHz, C_6D_6): δ 0.95 (dt, J = 15.6, 7.2 Hz, 12 H, PCH_2CH_3), 1.52 (q, J = 7.3 Hz, 6H, PCH_2CH_3), 1.4−2.6 (m, 12H, PCH_2CH_3), 1.5−2.0 (m, 2H, 8-CH_2), 1.8−2.4 (m, 2H, 7-CH_2), 2.5−2.7 (m, 2H, 1- and 4-C*H*═), 4.46 (brs, 2H, 2- and 3-C*H*═), 5.41 (m, 1H, 6-C*H*═), 6.23 (t, J = 9.3 Hz, 1H, 5-C*H*═), 6.75−7.50 (m, 15H, P*Ph*). $^{31}P\{^1H\}$ NMR (121.5 MHz, rt, C_6D_6): δ 22.4 (dd, J = 24, 6 Hz, 1P), 27.8 (dd, J = 24, 9 Hz, 1P), 31.2 (dd, J = 9, 6 Hz, 1P). $^{13}C\{^1H\}$ NMR (74.5 MHz, rt, C_6D_6): δ 9.26 (d, J = 3 Hz, PCH_2CH_3), 9.39 (d, J = 3 Hz, PCH_2CH_3), 10.0 (d, J = 4 Hz, PCH_2CH_3), 21.0 (s, 8-CH_2), 24.2 (d, J = 20 Hz, PCH_2CH_3), 24.9 (d, J = 20 Hz, PCH_2CH_3), 27.6 (s, 7-CH_2), 37.4 (dt, J = 39, 4 Hz, 1-C*H*═), 43.2 (d, J = 29 Hz, 4-C*H*═), 79.6 (s, 2- or 3-C*H*═), 81.1 (s, 3- or 2-C*H*═), 116.1 (brd, J = 5 Hz, 6-C*H*═), 138.7 (brs, *Ph*).

[L = P(n-Bu)$_3$ (4e)]. 1 (168.1 mg, 0.534 mmol) P(n-Bu)$_3$ (400 μl, 1.61 mmol) were used. **4e** was obtained as an almost pure yellow oil (403.2 mg, 0.495 mmol): yield 93%. This complex was characterized spectroscopically. Selected NMR data: ^{1}H NMR (300 MHz, C_6D_6): δ 0.92 (t, J = 7.2 Hz, 27H, $PC_3H_6CH_3$), 1.2−2.1 (m, 54H, $PC_3H_6CH_3$), 1.8−2.4 (8- and 7-CH_2, overlapped with signals due $PC_3H_6CH_3$), 2.46 (quint, J = 6.3 Hz, 1H, 4-C*H*═), 2.60 (q, J = 7.2 Hz, 1H, 1-C*H*═), 4.62 (brs, 1H, 3-C*H*═), 4.75 (m, 1H, 2-C*H* ═), 5.26 (m, 1H, 6-C*H*═), 6.15 (t, J = 9.3 Hz, 1H, 5-C*H*═). $^{31}P\{^1H\}$ NMR (121.5 MHz, 24 °C, C_6D_6): δ 9.5 (dd, J = 25, 6 Hz, 1P), 13.1 (dd, J = 25, 10 Hz, 1P), 18.1 (dd, J = 10, 6 Hz, 1P). $^{13}C\{^1H\}$ NMR (74.5 MHz, rt, C_6D_6): δ 14.1−14.3 (m, $P(CH_2)_3CH_3$), 21.0 (s, 8-CH_2), 25.1 (d, J = 10 Hz, $PCH_2(CH_2)_2CH_3$), 25.4 (d, J = 10 Hz, $PCH_2(CH_2)_2CH_3$), 25.6 (d, J = 10 Hz, $PCH_2(CH_2)_2CH_3$), 27.5−27.6 (m, $PCH_2(CH_2)_2CH_3$), 31.1 (d, J = 15 Hz, $PCH_2(CH_2)_2CH_3$), 31.6 (d, J = 13 Hz, $PCH_2(CH_2)_2CH_3$), 33.1 (d, J = 20 Hz, $PCH_2(CH_2)_2CH_3$), 36.6 (dt, J = 39, 4 Hz, 1-C*H*═), 43.2 (brd, J = 31 Hz, 4-C*H*═), 78.6 (s, 2- or 3-C*H*═), 79.6 (s, 3- or 2-C*H*═), 115.3 (d, J = 5 Hz, 6-C*H*═), 138.9 (brs, 5-C*H*═).

Characterization of RuH(η^5-C_8H_9)L_2 (5). The following (hydrido)ruthenium complexes RuH(η^5-C_8H_9)L_2 (**5**) were characterized by ^{1}H and $^{31}P\{^1H\}$ NMR spectra, homo-decoupling, and 2D-NMR measurements at low temperature, since they were obtained as an equilibrium mixture with **4**. They contained several isomers, and the complete assignment of the minor species was not feasible. Thus, only $^{31}P\{^1H\}$ NMR data and the hydride signals for the minor species are described.

[L = PEt_3 (5c)]. Major species (**5c**−**1**): ^{1}H NMR (300.4 MHz, −50 °C, $CD_3C_6D_5$): δ −14.1 (t, J = 26.9 Hz, 1H, Ru-*H*), 0.97 (dt, J = 15.6, 7.2 Hz, 18H, PCH_2CH_3), 1.61 (sept, J = 7.2 Hz, 6H, PCH_2CH_3), 3.20 (m, 3H, 2-C*H*═), 3.57 (brs, 1H, 5-C*H*═), 3.88 (brs, 1H, 1-C*H*═), 4.39 (t, J = 7.5 Hz, 1H, 3-C*H*═), 5.50 (brd, J = 7.5 Hz, 1H, 7-C*H*═), 5.79 (dt, J = 7.5, 4.2 Hz, 1H, 6-C*H*═). $^{31}P\{^1H\}$ NMR (121.6 MHz, −70 °C, $CD_3C_6D_5$): δ 30.0 (d, J = 15 Hz, 1P), 34.4 (d, J = 15 Hz, 1P). Minor species (**5c-2**): ^{1}H NMR (300.4 MHz, −60 °C, $CD_3C_6D_5$): δ −11.7 (dd, J = 33.0, 26.4 Hz, Ru-*H*). $^{31}P\{^1H\}$ NMR (121.6 MHz, −70 °C, $CD_3C_6D_5$): δ 28.4 (d, J = 24 Hz, 1P), 46.8 (d, J = 24 Hz, 1P). Minor species (**5c-3**): ^{1}H NMR (300.4 MHz, −70 °C, $CD_3C_6D_5$): δ −10.9 (t, J = 27.6 Hz, Ru-*H*). $^{31}P\{^1H\}$ NMR (121.6 MHz, −70 °C, $CD_3C_6D_5$): δ 30.3 (d, J = 24 Hz, 1P), 46.6 (obscured by overlapping with a signal due to **5c-2**). Minor species (**5c-4**): ^{1}H NMR (300.4 MHz, −60 °C, $CD_3C_6D_5$): δ −11.4 (dd, J = 34, 26 Hz, Ru-*H*). The $^{31}P\{^1H\}$ NMR spectrum was obscured. The ratio among **5c-1**, **5c-2**, **5c-3**, and **5c-4** based on the integration of their hydride resonances was 1:0.5: 0.25:0.08, respectively.

[L = PEt_2Ph (5d)]. Major species (**5d-1**): ^{1}H NMR (300.4 MHz, −20 °C, $CD_3C_6D_5$): δ −14.18 (t, J = 30 Hz, 1H, Ru-*H*), 0.6−1.0 (m, 12H, PCH_2CH_3), 1.93 (sext, J = 7.5 Hz, 1H, PCH_2CH_3), 1.96 (sext, J = 7.5 Hz, 1H, PCH_2CH_3), 2.21 (sext, J = 7.5 Hz, 2H, PCH_2CH_3), 2.29 (sext, J = 7.5 Hz, 1H, PCH_2CH_3), 2.30 (sext, J = 7.5 Hz, 1H, PCH_2CH_3), 2.51 (sext, J = 7.5 Hz, 2H, PCH_2CH_3), 3.00 (m, 1H, 2-C*H*═), 3.65 (m, 1H, 4-C*H*═), 3.7 (m, 1H, 5-C*H*═), 3.95 (m, 1H, 1-C*H*═), 4.67 (t, J = 7.5 Hz, 1H, 3-C*H*═), 5.43 (d, J = 6.8 Hz, 1H, 7-C*H*═), 5.75 (dt, J = 6.8, 4.5 Hz, 1H, 6-C*H*═), 8-CH_2 resonances (2H) were obscured by the overlapping with PEt_2Ph signals of **4d** and **5d**. $^{31}P\{^1H\}$ NMR (121.5 MHz, −20 °C, $CD_3C_6D_5$): δ 36.3 (d, J = 15 Hz, 1P), 38.9 (d, J = 15 Hz, 1P). Minor species (**5d-2**): ^{1}H NMR (300.4 MHz, −40 °C, $CD_3C_6D_5$): δ −11.28 (dd, J = 33.9, 24.0 Hz, Ru-*H*). $^{31}P\{^1H\}$ NMR (121.6 MHz, −60 °C, $CD_3C_6D_5$): δ 36.3 (d, J = 22 Hz, 1P), 48.0 (d, J = 22 Hz, 1P). Minor species (**5d-3**): ^{1}H NMR (300.4 MHz, −40 °C, $CD_3C_6D_5$): δ −10.53 (t, J = 29.1 Hz, Ru-*H*). $^{31}P\{^1H\}$ NMR (121.6 MHz −60 °C, $CD_3C_6D_5$): δ 47.2 (d, J = 18 Hz). The corresponding phosphorus peak was obscured. The ratio among **5d-1**, **5d-2**, and **5d-3** based on the integration of their hydride species was 1:0.13: 0.06, respectively.

[L = P(n-Bu)$_3$ (5e)]. ^{1}H NMR (300.4 MHz, 24 °C, C_6D_6): δ −11.5 (t, J = 32 Hz, 1H, Ru-*H*), 0.99 (t, J = 7.5 Hz, 18H, $PC_3H_6CH_3$), other signals were obscured by significant overlapping with **4e**. $^{31}P\{^1H\}$ NMR (121.6 MHz, 25 °C, C_6D_6): δ 23.6 (br, 1P), 27.6 (br, 1P).

Ru(η^4-C_8H_8)(PEt_3)$_3$ (6) and RuH(η^4-C_8H_{11})(PEt_3)$_2$ (7). Triethylphosphine (160 μl, 1.09 mmol) was added to a solution of **2** (82.3 mg, 0.261 mmol) in 2 mL of toluene. The reaction mixture was stirred at 50 °C for 3 days. After removal of volatile materials, the NMR spectrum of the residual red oil shows a crude mixture of **6** and **7** in 1:1 ratio. Fractional crystallization from pentane gave red crystals of **6** (18.7 mg, 0.0334 mmol): yield 13%. Heating of the isolated **4c** in benzene at 70 °C for 100 h also caused disproportionation reaction of the η^4-C_8H_{10} moiety to give a mixture of Ru(η^4-C_8H_8)(PEt_3)$_3$ (**6**) and RuH(η^5-C_8H_{11})(PEt_3)$_3$ (**7**) in 43 and 42% yields, respectively. Complex **6** was characterized by X-ray analysis and NMR spectrum. ^{1}H NMR (300.4 MHz, 23 °C, C_6D_6): δ 0.88

(brs, 27H, PCH_2CH_3), 1.54 (brs, 18H, PCH_2CH_3), 5.22 (s, 8H, C_8H_8). $^{31}P\{^1H\}$ NMR (121.5 MHz, 24 °C, C_6D_6): δ 27.7 (s). On the other hand, complex **7** was characterized from the NMR spectrum of a mixture of **6** and **7**. ^1H NMR (300.4 MHz, 24 °C, C_6D_6): δ −11.6 (t, J = 31 Hz, 1H, Ru-*H*), 0.5−2.2 (m, 36H, PEt, 6-, 7-, and 8-CH_2), 2.49 (brs, 2H, 1- and 5-C*H*═), 3.45 (brs, 1H, 3-C*H*═), 4.85 (brs, 2H, 4- and 2-C*H*═). ^1H NMR (300.4 MHz, 20.2 °C, acetone-d_6): −11.78 (t, J = 32.1 Hz, 1H, Ru-*H*), 0.33 (q, J = 13.8 Hz, 1H, *H*-7*exo*), 1.0 (*H*-7*endo*, overlapped with PEt_3), 1.3−2.0 (*H*-6 + *H*-8, overlapped with PEt_3), 2.2 (m, 2H, *H*-1 + *H*-5), 4.75−4.55 (m, 2H, *H*-2 + *H*-4), 5.18 (t, J = 6.6 Hz, 1H, *H*-3).

Preparation of Ru(η^4-bicyclo[4.2.0]octa-2,4-diene)L_3 (8). [L = PEt_3 (8a)]. Triethylphosphine (34 μL, 0.23 mmol) was added to a solution of **1** (24.2 mg, 0.0767 mmol) in 600 μL of benzene. The reaction mixture was heated at 70 °C for 88 h to give a mixture of **8a** (0.051 mmol, 67%), Ru(C_8H_{12})(C_8H_{10})-(PEt_3) (0.011 mmol, 14%), and **7** (0.0092 mmol, 12%). Complex **8a** was isolated by recrystallization from acetone (16.4 mg, 0.0291 mmol): 38% yield. Anal. Calcd for $C_{26}H_{55}P_3Ru$: C, 55.59; H, 9.87. Found: C, 55.99; H, 9.89. ^1H NMR (300.4 MHz, −60 °C, $CD_3C_6D_5$): δ 0.83 (br, 18H, PCH_2CH_3), 1.09 (dt, J = 12.6, 6.6 Hz, 9H, PCH_2CH_3), 1.30 (brm, 6H, PCH_2CH_3), 1.40 (brm, 6H, PCH_2CH_3), 1.62 (br, 6H, PCH_2CH_3), 1.75 (brs, 2H, *endo*-6- and 7-C*H*H), 2.22 (brs, 2H, *exo*-6- and 7-C*H*H), 2.52 (brs, 4H, 1-, 4- and 5- and 8-C*H*), 4.85 (brs, 2H, 2- and 3-C*H*). $^{31}P\{^1H\}$ NMR (121.5 MHz, −60 °C, $CD_3C_6D_5$): δ 18.8 (d, J = 9 Hz, 2P), 29.5 (t, J = 9 Hz, 1P).

[L = PEt_2Ph (8b)]. Diethylphenylphosphine (520 μl, 2.98 mmol) was added to a solution of **1** (230.7 mg, 0.731 mmol) in 3 mL of toluene. The reaction mixture was stirred at 50 °C for 4 days. After volatile materials were removed, the residual red oil was crystallized from acetone to give a yellow powder for **8b** (236.5 mg, 0.3360 mmol): yield 46%. Anal. Calcd for $C_{38}H_{55}P_3Ru$: C, 64.66; H, 7.85. Found: C, 64.51; H, 7.83. ^1H NMR (300.4 MHz, 26 °C, C_6D_6): δ 0.7 (brs, 18H, PCH_2CH_3), 1.59 (quint, J = 4.8 Hz, 2H, *endo*-6- and 7-C*H*H), 1.8 (brs, 12H, PCH_2CH_3), 2.08 (qui, J = 4.5 Hz, 1H, *exo*-6- or 7-C*H*H), 2.09 (qui, J = 5.1 Hz, 1H, *exo*-6- or 7-C*H*H), 2.37 (m, 2H, 1- and 4-C*H*), 2.57 (brs, 2H, 5- and 8-C*H*), 4.60 (m, 2H, 2- and 3-C*H*), 6.93−7.33 (brs, 15H, P*Ph*). $^{31}P\{^1H\}$ NMR (121.5 MHz, 26 °C, C_6D_6): δ 26.9 (brs, 2P), 36.2 (brs,1P).

Reaction of Ru(η^4-C_8H_{10})(PEt_3)$_3$ (4c) with Vinyl Propionate. In Situ NMR Studies. A 5 mm NMR tube was charged first with a solid sample of Ru(η^4-C_8H_{10})(PEt_3) (**4c**) (15.8 mg, 0.0281 mmol) under nitrogen atmosphere and C_6D_6 (400 μL) was added. Then, vinyl propionate (3 μL, 0.03 mmol) was added. The NMR tube was placed in a oil bath at 50 °C, and ^1H and $^{31}P\{^1H\}$ NMR spectra were acquired frequently until complete formation of Ru(η^1-C_2H_3)(η^2-OCOEt)(PEt_3)$_3$[25] (89% yield after 10 h, using ferrocene as an internal standard).

Crystallographic Study of 3b, 4c, 6, and 8b. Crystals suitable for an X-ray diffraction study were obtained from hexane (**3b** and **4c**) or pentane (**6** and **8b**) solutions at −10 °C. The crystal data and experimental data for **3b**, **4c**, **6**, and **8b** are summarized in Table 1. Diffraction data were obtained with a Rigaku AFC-7R diffractometer. The reflection intensities were monitored by three standard reflections at every 150 measurements. The data for **3b**, **4c**, **6**, and **8b** were corrected for Lorentz and polarization effects. A linear correction factor was applied in **3b** and **6** due to a decrease of the standards over the course of the data collection by 13.6 and 34.9%, respectively. An empirical absorption correction based on ψ-scans was applied to **8b**, resulting in transmission factors ranging from 0.85 to 0.99. All structures were solved by Patterson methods and expanded using Fourier techniques. All non-hydrogen atoms were refined anisotropically in **3b**, **4c**, **6**, and **8b**. Hydrogen atoms were included in all cases but not refined. All calculations were performed using the teXan[26] crystallographic software package of Molecular Structure Corporation. Selected bond distances and angles are given in Tables 2, 3, 5, and 6. The C(5)═C(6) bond distance [1.29(2) Å] of the cyclooctatriene moiety in **4c** is slightly shorter than the ordinal C═C bond. Detailed analysis of the Laue symmetry for this crystal shows an *mmm* crystal system, and the extinction rule appearing in the data collection table indicates a highly symmetric space group, *Iba*2 (N = 8). The most likely reason for the observation of the inappropriate bond distance is due to possible disorder in the highly symmetric unit cell, although such disorder could not be found in the differential Fourier map. By these considerations we avoided detailed discussion of the bond distances and angles except the overall structure for **4c**.

Acknowledgment. The work was partially supported by the Proposal-Based New Industry Creative Type Technology R&D Promotion Program from the New Energy and Industrial Technology Development Organization (NEDO) and a Grant-in-Aid for Scientific Research from the Ministry of Education, Science, Sports and Culture, Japan. We thank Ms. C. Nagata for the elemental analysis.

Supporting Information Available: Tables of crystallographic data, atom coordinates, thermal parameters, and bond distances and angles for **3b**, **4c**, **6**, and **8b**. This material is available free of charge via the Internet at http://pubs.acs.org.

OM991014K

(25) Planas, J. G.; Marumo, T.; Ichikawa, Y.; Hirano, M.; Komiya, S. *Dalton Trans.*, in press.
(26) *teXan*, Crystal Structure Analysis Package; Molecular Structure Coorporation, 1985 and 1992.